IOPscience iopscience.iop.org

Home Search Collections Journals About Contact us My IOPscience

Photoluminescence of F-passivated ZnO nanocrystalline films made from thermally oxidized ZnF_2 films

This article has been downloaded from IOPscience. Please scroll down to see the full text article.

2004 J. Phys.: Condens. Matter 16 5143

(http://iopscience.iop.org/0953-8984/16/28/032)

View the table of contents for this issue, or go to the journal homepage for more

Download details:
IP Address: 159.226.165.151
The article was downloaded on 05/09/2012 at 04:54

Please note that terms and conditions apply.

INSTITUTE OF PHYSICS PUBLISHING JOURNAL OF PHYSICS: CONDENSED MATTER

J. Phys.: Condens. Matter **16** (2004) 5143–5150 PII: S0953-8984(04)78219-3

Photoluminescence of F-passivated ZnO nanocrystalline films made from thermally oxidized ZnF_2 films

H Y Xu[1,2], Y C Liu[1,2,4], J G Ma[2], Y M Luo[1], Y M Lu[2], D Z Shen[2], J Y Zhang[2], X W Fan[2] and R Mu[3]

[1] Centre for Advanced Opto-Electronic Functional Material Research, Northeast Normal University, Changchun 130024, People's Republic of China
[2] Key Laboratory of Excited State Processes, Changchun Institute of Optics, Fine Mechanics and Physics, Chinese Academy of Sciences, 16-Dongnanhu Avenue, Changchun 130033, People's Republic of China
[3] Centre for Photonic Materials and Devices, Fisk University, Nashville, TN 37028, USA

E-mail: ycliu@nenu.edu.cn

Received 22 March 2004, in final form 13 May 2004
Published 2 July 2004
Online at stacks.iop.org/JPhysCM/16/5143
doi:10.1088/0953-8984/16/28/032

Abstract
F-passivated ZnO nanocrystalline films were prepared by thermal oxidation of ZnF_2 films. ZnF_2 films were deposited on a Si wafer by the electron beam evaporation technique. X-ray diffraction and x-ray photoelectron spectroscopy were used to study the structural changes of ZnF_2 as a function of oxidation temperature. When the ZnF_2 film was oxidized at 400 °C for 30 min, a polycrystalline hexagonal wurtzite structure of ZnO:F was obtained. The room temperature photoluminescence spectrum of the ZnO:F film showed a strong near band edge ultraviolet emission located at 379 nm with a narrow linewidth of 70 meV and a very weak visible emission associated with deep level defects. The results demonstrated that the presence of residual F ions in ZnO nanocrystalline film can dramatically decrease the visible emission and increase the ultraviolet emission of ZnO. On the basis of the experimental findings, two possible mechanisms are proposed: (1) the residual F ions in the film occupy the lattice sites of Vo^* centres (the oxygen vacancies with one electron) inside the ZnO nanocrystals, which results in an appreciable decrease in visible emission and (2) some of the F ions also passivate ZnO nanocrystal surface states, which prevents the holes in the valence band from being trapped in surface states and then tunnelling back into nanocrystals to combine with Vo^* to form Vo^{**} centres ($Vo^* + h \rightarrow Vo^{**}$) which are another source of visible emission.

[4] Author to whom any correspondence should be addressed.

 © 2004 IOP Publishing Ltd Printed in the UK

1. Introduction

Zinc oxide (ZnO), a semiconductor with a large exciton binding energy (60 meV) and wide band gap (3.37 eV), has attracted much interest as regards piezoelectrical, electro-optical, acousto-optical and chemical and biological sensory applications. Recently, it has attracted much more attention as regards applications in optoelectronic devices due to a breakthrough in the preparation of homostructural ZnO p–n junctions [1], transparent ZnO thin-film transistors [2] and low dimensional ZnO nanostructures [3–6]. The photoluminescence (PL) spectrum of ZnO usually shows a near band edge ultraviolet (UV) emission and a visible emission. The latter is associated with deep level defects and surface state related emissions. For improperly prepared ZnO polycrystalline films, defect related deep level emission dominates in a PL spectrum, which precludes various applications, for example, UV luminescence devices [7] and unconventional random lasers [8, 9]. It is known that the UV luminescence of ZnO is due to free and bound exciton emission [6, 9], while the visible emission is thought to be defect related emission. However, the exact emission mechanisms are not thoroughly understood and may still be controversial. In the literature, various mechanisms have been proposed. These include the involvement of oxygen vacancies [10–12] and interstitial oxygen [13, 14], zinc vacancies and interstitial zinc [15], and even Cu ion impurities [16]. The latest investigation [17] indicates that the oxygen vacancy without an electron (Vo^{**}) can also serve as a recombination centre for the visible emission. In the latter case, the holes in the valence band are believed to be trapped by the surface states of ZnO nanocrystals first. Then the surface-trapped holes tunnel back inside the particles to combine with the oxygen vacancies Vo^{*} to form Vo^{**} centres. This model indicates that the Vo^{*} centres and the surface defects of ZnO nanocrystals play important roles in the formation of the visible emission centres (Vo^{**}).

In order to fully explore the potential of ZnO nanocrystals for optoelectronic applications, passivation may be the most effective way to mitigate or eliminate the visible emission, such as by employing organic capping or proper doping techniques [18, 19]. Since the ionic radius of F is similar to that of O, it is believed that using F ions can prevent a large lattice distortion which would degrade the quality of the ZnO. In this paper, we have developed an experimental method for incorporating F ions into ZnO nanocrystalline films via a reverse doping process—oxidation of ZnF_2—and demonstrate how the F ions can be used to reduce or even eliminate visible emissions from ZnO nanocrystals.

2. Experiment

Zinc fluoride (ZnF_2, 5N) was used as the material for electron beam evaporation. A ZnF_2 thin film was deposited onto a Si(100) substrate. The substrate was pre-cleaned by a standard RCA method. The evaporation pressure was kept at 5×10^{-5} Pa, and the temperature of the substrate was 400 °C. The average deposition rate is 80 nm min^{-1}. After the deposition, the sample was thermally oxidized at temperatures of 300, 400 and 500 °C in an O_2 atmosphere. A 30 min oxidation period was used at each temperature. The film thickness was measured using an ellipsometer. The thickness was confirmed to be about 790 nm for the as-deposited ZnF_2 films. To characterize the structure of the film, a set of x-ray diffraction (XRD) spectra was collected with a D/max-RA x-ray spectrometer (Rigaku) with the Cu Kα line of 1.54056 Å. X-ray photoelectron spectroscopy (XPS) measurements were also carried out with a VG ESCALAB MK II x-ray photoemission spectrometer to identify the chemical compositions of the films. For optical characteristics, microphotoluminescence measurements were conducted with a J–Y UV Lamb micro-Raman spectrometer with a back-scattering configuration. A He–Cd laser at 325 nm was used as an excitation source.

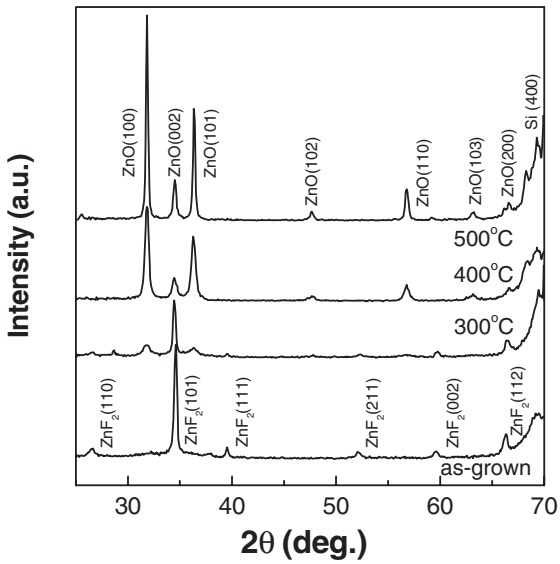

Figure 1. XRD spectra of the as-grown ZnF_2 and the thin films annealed at different temperatures.

3. Results and discussion

Figure 1 shows XRD spectra (θ–2θ) of an as-deposited ZnF_2 sample and the samples annealed at different temperatures from 300 to 500 °C. For the as-grown sample, the diffraction peaks reflect a typical ZnF_2 film with a rutile structure, indicating the formation of a polycrystalline ZnF_2 film. When the sample was annealed at 300 °C, three new diffraction peaks in the XRD spectra appeared at $2\theta = 31.80°$, 36.33° and 47.77°, which correspond to the (100), (101) and (102) diffraction lines of ZnO with a hexagonal wurtzite structure, respectively. XRD results clearly showed a coexistence form with both ZnF_2 and ZnO phases. This is a result of a partial transformation from ZnF_2 to ZnO via thermal oxidation. When the sample was annealed at 400 °C for 30 min, all of the diffraction peaks associated with ZnF_2 disappeared and a single phase of ZnO resulted. The XRD spectra also indicated that the film is made of ZnO nanocrystals with no preferred orientation. As the annealing temperature was increased to 500 °C, the diffraction peaks of the ZnO film became sharper and more intense due to the increased particle size as well as the improved crystal quality.

To evaluate the average grain size of the ZnO film, the Scherrer formula [20] was used:

$$D = \frac{0.9\lambda}{B\cos(\theta_B)}$$

where λ, θ_B and B are the x-ray wavelength (1.540 56 Å), the Bragg diffraction angle and the full width at half-maximum of the diffraction peak, respectively. The calculated average grain sizes of the as-grown ZnF_2 and ZnO films obtained via oxidation at 400, 500 °C were 22, 18 and 32 nm, respectively.

High resolution XPS spectra of the as-grown ZnF_2 film and the films annealed at three different temperatures are shown in figure 2. The binding energy scale was calibrated using the C 1s peak as a reference energy marker (284.6 eV). Figure 2(a) gives typical XPS spectra of the Zn $2p_{3/2}$ core level. The core lines of Zn 2p exhibited a symmetric Gaussian lineshape indicating a single component of Zn^{2+} ions. For the ZnO film annealed at 500 °C, the binding

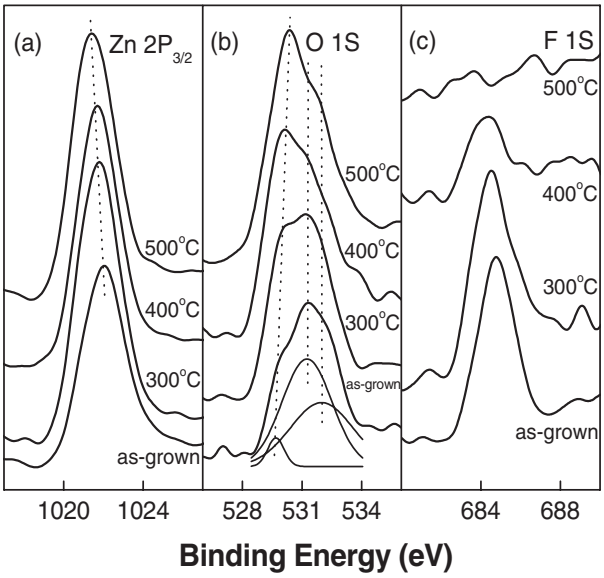

Figure 2. XPS spectra ((a) Zn 2p, (b) O 1s, (c) F 1s) of the as-grown ZnF_2 and the thin films annealed at different temperatures.

energy of Zn $2p_{3/2}$ in Zn–O appeared at 1021.40 eV, which was in good agreement with the value for Zn $2p_{3/2}$ in bulk ZnO (1021.49 eV). For the as-grown ZnF_2 film, the binding energy of Zn $2p_{3/2}$ in Zn–F is at 1022.00 eV. An energy red-shift upon oxidation suggests a structural transformation from ZnF_2 to ZnO. Because F ions in the as-grown ZnF_2 have stronger attraction to electrons from the Zn core than the O in ZnO, the electron screening effect of Zn^{2+} in ZnF_2 is weaker than that of Zn^{2+} in ZnO. As a result, the Zn $2p_{3/2}$ has a larger binding energy in ZnF_2 than in ZnO. Figure 2(b) shows the XPS spectra of the O 1s core level. Judging from the XPS spectra obtained for three different temperatures, the O 1s spectra may be described as the superpositions of three bands. The best curve fitting suggests that the three peaks are centred at 530.15, 531.20 and 532.25 eV, respectively. Among these, the strongest band is located at 532.25 eV which can be attributed to weakly bound oxygen on the surface of the film [21]. Because of the residual oxygen present during deposition and the oxygen atmosphere of the annealing treatments, it is reasonable to assign this band to surface absorbed O_2. The band at 531.20 eV is argued to originate from the O^{2-} associated with F^- ions. The component at 530.15 eV was attributed to O^{2-} ions in Zn–O [21]. The intensity of this component represents the amount of oxygen atoms in a fully oxidized stoichiometric environment. For the as-grown sample, there was a little O_2 remaining in the growth chamber. When the ZnF_2 was evaporated and deposited on the substrate, the remaining O_2 could be trapped into the crystal lattice of ZnF_2. Therefore, weak XPS intensity of O^{2-} ions in O–Zn–O is present for the as-grown ZnF_2 film. As the annealing temperature increased, the degree of the oxidation was enhanced. Thus, the intensity of this peak increased, as illustrated in figure 3. Figure 2(c) shows the XPS spectra of the F 1s core level. The binding energy located at 684.6 eV was attributed to F^- in Zn–F. As expected, this band intensity decreased prominently with increase of the annealing temperature. Figure 3 is the plot produced to highlight the decrease of F concentration and increase of O concentration. Clearly, as temperature is increased, the O concentration increases monotonically at the expense of a decrease of the F concentration. When the annealing temperature reached 500 °C, the peak of F 1s disappeared. That is, the

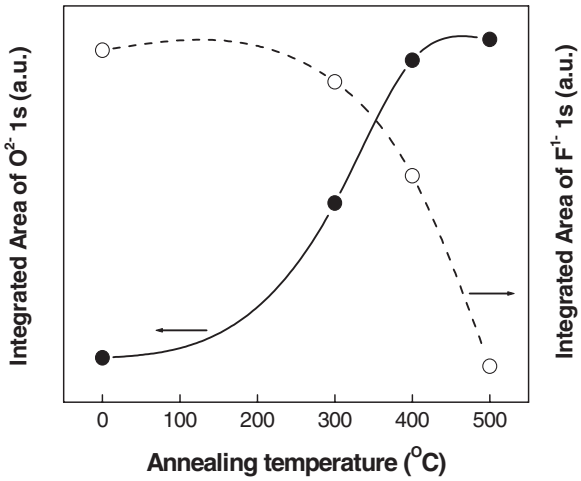

Figure 3. The integrated area of O^{2-} 1s in ZnO (530.15 eV) and F^{1-} s (684.6 eV) in XPS spectra as a function of the annealing temperature.

system reaches near complete oxidation. For 400 °C, a calculation has been carried out to obtain atomic composition by using the integrated peak area and sensitivity factors. The results show that the percentage concentrations of Zn, O and F are 51.8%, 45.2% and 3.0%, respectively. The XRD and XPS results confirm that F-doped ZnO and undoped ZnO are formed at annealing temperatures of 400 and 500 °C, respectively.

Photoluminescence (PL) spectroscopy is an effective technique for characterizing the crystal quality of ZnO. The PL spectrum of routinely prepared ZnO thin film contains two emission bands; that is, a UV emission at ∼375 nm and a visible emission at ∼500 nm. The former is due to free exciton emission because the bound excitons are usually thermally ionized at room temperature [6, 9, 22], while the latter is usually attributed to structure defects [10–12, 17]. Figure 4 shows the room temperature normalized PL spectra of the as-grown ZnF_2 film and the film annealed at the aforementioned three different temperatures. For the as-grown sample, an emission centred at 360 nm could be detected, although it was very weak. This emission may be due to a trace of oxygen incorporated into the crystal lattice of ZnF_2 during the deposition process. Increasing annealing temperature favours diffusion of oxygen in the crystal and therefore increases the UV emission. As the annealing temperature increased from 300 to 500 °C, the peak positions of the UV PL were located at 375, 379, 382 nm, sequentially (see also the inset in figure 4). The red-shift of the peak position may be attributed to many factors such as the quantum confinement effect, the stress effect and the Burstein–Moss effect [6, 23]. It is also interesting to note that for the sample annealed at 400 °C, the UV PL peak showed a smaller full width at half-maximum (FWHM), 70 meV, than the higher and lower temperature ones. It is also narrower than the 98 meV observed for a ZnO epilayer grown on CaF_2 by MBE [24]. One of the logical explanations may be a narrow distribution of ZnO nanocrystal size and the effective elimination of structural defects. The PL spectrum obtained from the sample that was thermally oxidized at 500 °C showed a broader linewidth (FWHM = 96 meV) of the UV PL peak and a detectable visible emission providing evidence of a deep level of defects present in the sample. The results provide further proof that the F ions present in ZnO serve as dopants for defect passivation.

It is known that ZnO semiconductor has several kinds of structural defects that include interstitial atoms and vacancies. These defects can be anionic or cationic. Electron

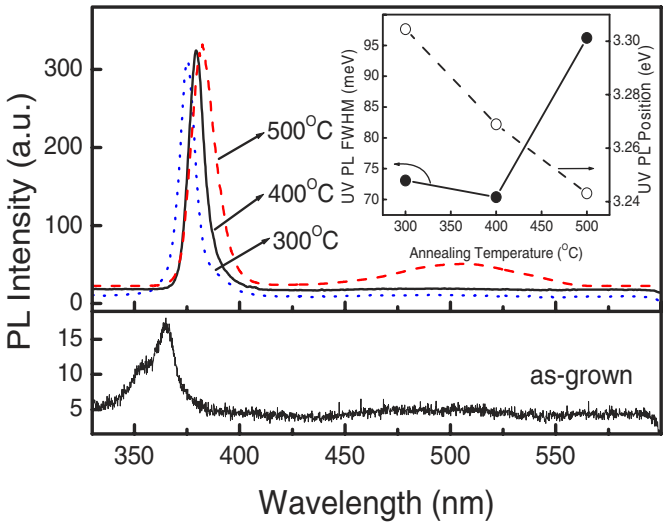

Figure 4. Room temperature PL spectra of the as-grown ZnF_2 films and the thin films annealed at different temperatures. The inset shows the UV PL peak position and the linewidth (FWHM) as a function of annealing temperature.

(This figure is in colour only in the electronic version)

paramagnetic resonance (EPR) studies have shown that the oxygen vacancies containing one electron (Vo*) are the predominant paramagnetic defects [25, 26]. The visible emission is the result of the recombination of an electron from the conduction band with the Vo* centre [27], which has an effective monovalent positive charge with respect to the regular O^{2-} sites. However, recent investigations have suggested that the Vo* are not the direct recombination centres for the visible emission of ZnO [17, 19]. Rather, the visible emission is due to the recombination of a shallowly trapped electron with a Vo** centre—that is, an oxygen vacancy containing no electrons and having an effective divalent positive charge with respect to the normal O^{2-} site. The relaxation process may be as illustrated in figure 5. In this schematic diagram, the energy band structure of ZnO, the deep trap levels (Vo*/Vo**) and the energy distribution of the O_s^{2-}/O_s^{-} surface system are shown. For simplicity, the shallow trapping of a photogenerated electron is not shown. The UV emission can be represented by an electron in the conduction band recombining with a hole in the valence band. The visible emission is a three-step process. Upon photon excitation, holes in the valence band inside the nanocrystal can first diffuse to the surface and be trapped by surface defects. Then, some of surface-trapped holes will find their way tunnelling back inside the nanocrystal to recombine with Vo* to form Vo**. The visible emission is the recombination of a shallowly trapped electron with a deeply trapped hole in a Vo** centre. On the basis of this argument, both Vo* centres and surface states of ZnO nanocrystals are seen to play important roles in the visible emission. Suppressing any one of the defects or both will lead to the elimination of the visible emission. Therefore, it is conceivable that there may be two quenching mechanisms for visible emission in the current case:

(a) in the case of incomplete oxidation, F atoms may occupy the lattice sites of the Vo* centres—thus, the probabilities of forming Vo** centres are eliminated;
(b) because of the large surface-to-volume ratio of nanocrystal, there exist many dangling bonds on the surfaces of ZnO nanocrystals.

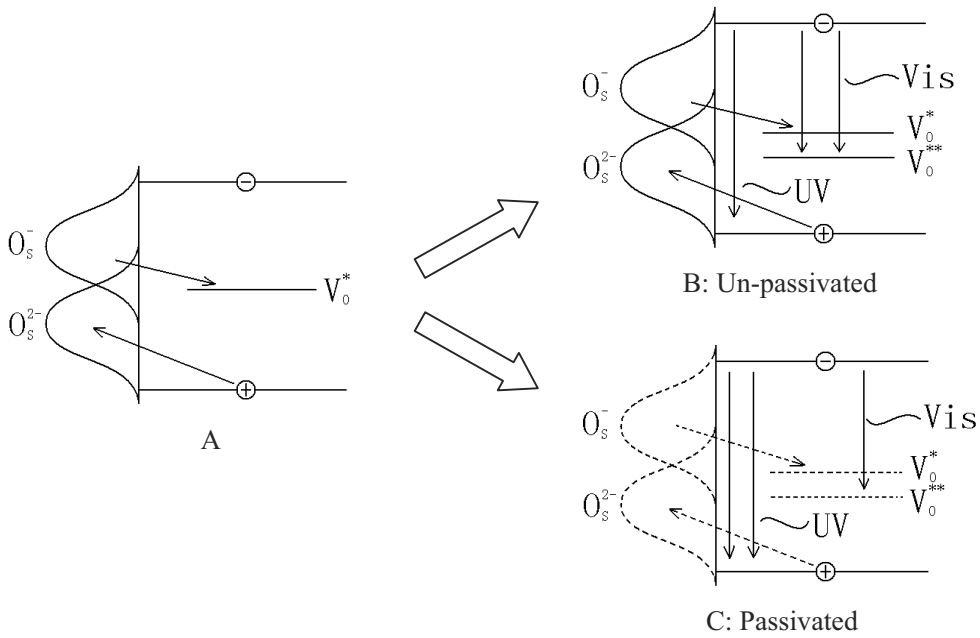

Figure 5. A shows a schematic overview of the relaxation processes of a photoexcited ZnO particle; B shows the mechanism of visible emission in undoped ZnO thin films; C shows the mechanism of visible emission quenched in F-passivated ZnO thin films.

These dangling bonds are the sites that can trap O^{2-} and O^- ions to form the O_s^{2-}/O_s^- on the surface [28]. O_s^{2-}/O_s^- surface sites are the major traps for the holes diffused out from inside the nanocrystals. The presence of the F ions has passivated these defects on the surface of ZnO nanocrystals, which, in turn, prevents hole trapping and blocks the pathway for Vo^{**} centre formation. Thus, visible emission is dramatically reduced. This explanation can also be supported by some of the previous work on the luminescence of ZnO nanocrystals in which the ions, such as Fe^{2+} and I^-, were found to be efficient quenchers of the visible luminescence [27, 29, 30]. Moreover, F passivation can also decrease the nonradiative combination on the surface of ZnO nanocrystals.

4. Conclusion

A ZnF_2 thin film was deposited on a Si(100) substrate by electron beam evaporation. Via thermal oxidation of the ZnF_2 films at various temperatures ranges from 300 to 500 °C in O_2 ambient, polycrystalline ZnO:F thin film with a wurtzite structure was formed. The XRD and XPS results gave insight into the process of transformation from ZnF_2 to ZnO. The PL results demonstrated that the F passivation can eliminate the visible emission of ZnO. Passivation mechanisms were proposed:

(1) inside the nanocrystals, F atoms occupy the lattice sites of the Vo^* centres, which decreases the probability of forming visible emission centres (Vo^{**});
(2) on the surface of nanocrystals, the residual F passivates the surface defect states; thus, the pathway for forming Vo^{**} centres is blocked.

The aforementioned factors contribute to the decrease of visible emission in ZnO.

Acknowledgments

This work was supported by the National Natural Science Foundation of China (60176003, 60376009 and 60278031): the Excellent Researcher to Go Beyond the Century of the Ministry of Education of China.

References

[1] Ryu Y R, Lee T S, Leem J H and White H W 2003 *Appl. Phys. Lett.* **83** 4032
[2] Carcia P F, McLean R S, Reilly M H and Nunes G Jr 2003 *Appl. Phys. Lett.* **82** 1117
[3] Kong X Y and Wang Z L 2004 *Appl. Phys. Lett.* **84** 975
[4] Kim T W, Kawazoe T, Yamazaki S, Ohtsu M and Sekiguchi T 2004 *Appl. Phys. Lett.* **84** 3358
[5] Chik H, Liang J, Cloutier S G, Kouklin N and Xu J M 2004 *Appl. Phys. Lett.* **84** 3376
[6] Liu Y C, Xu H Y, Mu R, Henderson D O, Lu Y M, Zhang J Y, Shen D Z, Fan X W and White C W 2003 *Appl. Phys. Lett.* **83** 1210
[7] Aoki T, Hatanaka Y and Look D C 2000 *Appl. Phys. Lett.* **76** 3257
[8] Cao H, Xu J Y, Seeling E W and Chang R P H 2000 *Appl. Phys. Lett.* **76** 2997
Cao H, Xu J Y, Seeling E W and Chang R P H 2000 *Phys. Rev. Lett.* **84** 5584
[9] Tang Z K, Wong G K L, Yu P, Kawasaki M, Ohtomo A, Koinuma H and Segawa Y 1998 *Appl. Phys. Lett.* **72** 3270
[10] Kasai P H 1963 *Phys. Rev.* **130** 989
[11] Kroger F A and Vink H J 1954 *J. Chem. Phys.* **22** 250
[12] Prosanov I Y and Politov A A 1995 *Inorg. Mater.* **31** 663
[13] Hahn D and Nink R 1965 *Phys.: Condens. Mater.* **3** 331
[14] Liu M, Kitai A H and Mascher P 1992 *J. Lumin.* **54** 35
[15] Bylander E G 1978 *J. Appl. Phys.* **49** 1188
[16] Dingle R 1969 *Phys. Rev. Lett.* **23** 579
[17] Dijken A V, Meulenkamp E A, Vanmaekelbergh D and Meijerink A 2000 *J. Phys. Chem.* B **104** 1715
[18] Yang C L, Wang J N, Ge W K, Guo L, Yang S H and Shen D Z 2001 *J. Appl. Phys.* **90** 4489
[19] Zhang X T, Liu Y C, Zhang J Y, Lu Y M, Shen D Z, Fan X W and Kong X G 2003 *J. Cryst. Growth* **254** 80
[20] Cullity B D 1978 *Elements of X-ray of Diffractions* (Reading, MA: Addison-Wesley) p 102
[21] Chen M, Wang X, Yu Y H, Pei Z L, Bai X D, Sun C, Huang R F and Wen L S 2000 *Appl. Surf. Sci.* **158** 134
[22] Cho S, Ma J, Kim Y, Sun Y, Wong G K L and Ketterson J B 1999 *Appl. Phys. Lett.* **75** 2761
[23] Fujihara S, Suzuki A and Kimura T 2003 *J. Appl. Phys.* **94** 2411
[24] Ko H J, Chen Y F, Zhu Z, Yao T, Kobayashi I and Uchiki H 2000 *Appl. Phys. Lett.* **76** 1905
[25] Anpo M and Kubokawa Y 1984 *J. Phys. Chem.* **88** 5556
[26] Vanheusden K, Seager C H, Warren W L, Tallant D R and Voigt J A 1996 *Appl. Phys. Lett.* **68** 403
[27] Kamat P V and Patrick B 1992 *J. Phys. Chem.* **96** 6829
[28] Schoenmakers G H, Vanmaekelbergh D and Kelly J J 1996 *J. Phys. Chem.* **100** 3215
[29] Bahnemann D W, Kormann C and Hoffmann M R 1987 *J. Phys. Chem.* **91** 3789
[30] Harada Y and Hashimoto S 2003 *Phys. Rev.* B **68** 045421